Facile electrodeposition of superhydrophobic aluminum stearate thin films on copper substrates for active corrosion protection

Wei Xu, Karthikeyan Rajan, X. Grant Chen, Dilip K. Sarkar

PII: S0257-8972(19)30223-3
DOI: https://doi.org/10.1016/j.surfcoat.2019.02.070
Reference: SCT 24387

To appear in: *Surface & Coatings Technology*

Received date: 25 November 2018
Revised date: 15 February 2019
Accepted date: 20 February 2019

Please cite this article as: W. Xu, K. Rajan, X.G. Chen, et al., Facile electrodeposition of superhydrophobic aluminum stearate thin films on copper substrates for active corrosion protection, Surface & Coatings Technology, https://doi.org/10.1016/j.surfcoat.2019.02.070

Facile electrodeposition of superhydrophobic aluminum stearate thin films on copper substrates for active corrosion protection

Wei Xu, Karthikeyan Rajan, X.Grant Chen, Dilip.K. Sarkar*

University Research Centre on Aluminium (CURAL)andAluminium Research Centre-REGAL,
University of Québec at Chicoutimi (UQAC), 555 Boulevard de l'Université, Chicoutimi, Quebec, G7H 2B1, Canada

*(*Corresponding author: dsarkar@uqac.ca)*

Abstract:

A facile aluminum based superhydrophobic thin films were electrodeposited by mixing aluminum isopropoxide (AlO_x) with stearic acid (SA) onto the copper substrates via one-step method. The energy dispersive X-ray spectroscopy (EDS)attenuated total-reflectance Fourier Transmission infrared spectroscopy (ATR-FTIR) were used to confirm the presence of Al, C, and O as well as COO-Al and C-H bonds in the thin film. The water-roll off properties were analyzed by measuring the contact angle to study the superhydrophobic nature of fabricated films. Results show that superhydrophobicity with the water contact angle of 161 ± 1° and the contact angle hysteresis of 2± 1° were obtained with respect to the AlO_x/SA molar ratio of 0.33. The morphology of the fabricated thin films consisted of uniform porous structures with surface roughness (rms) of 3 μm on the copper substrate. The addition of stearic acid plays an important role for the superhydrophobic property. Furthermore, the thin films and their anticorrosion behavior were investigated using 3.5 wt.% corrosive aqueous NaCl electrolyte solution. The polarization resistance of the thin

film is found to be 962 kΩ·cm^2 as characterized by Tafel. Similarly, impedance value of 10 MΩ·cm^2 was obtained from Electrochemical Impedance Spectroscopy (EIS). A simple fabrication of water-repellent superhydrophobic aluminum-based coating endues extremely high active in corrosion protection.

Keywords: Copper (Cu); superhydrophobic; stearic acid; electrodeposition; anticorrosion

Introduction:

Growing interests in the wettability of a solid surface have a wide range of implications in the field of science and engineering. Superhydrophobicity is considered as an important property for the extreme state of surface wettability. These surfaces exhibit high water repellency, where the water drops bead up on the surface (contact angle more than 150°), and the droplet readily slide away from the surface(small contact angle hysteresis) [1,2]. A micro or nanostructured rough surface texture and a nonpolar surface chemistry having low surface energy are the two essential parameters which help trap a thin layer of air that limits the interactions between solid and liquid surface [3]. Superhydrophobic surfaces have achieved much attention in many industrial applications, such as anti-fogging[4], anti-frosting[5], anti-icing[6], self-cleaning [7], superamphiphobic, omniphobic [8], drag reduction [9], biomedical uses[10] as well as anticorrosion applications [11].The physico-chemical interaction between a metal and its environment alters its surface chemical properties, which referred as corrosion[12]. The concept of preparing superhydrophobic surfaces creates enormous chances within the area of corrosion inhibition for metals and alloys.

Due to their self-cleaning property and water roll-off performance, superhydrophobic coatings provide an approach to slow down the corrosion process of metals and thus prevent the metal surfaces underneath from further corrosion[13].

Several surface treatments methods such as anodization [14], electroplating[15], electroless plating[16], spray coating[17], etc. have been explored for improving performance and longevity of metal substrates. Among current industry strategies for combatting corrosion, the transformation of hydrophilic metal substrate into anticorrosive surface via superhydrophobic coatings is considered an excellent alternative for metal protection, particularly for copper substrate against corrosion [18]. Copper (Cu) is an abundant material in nature. Due to its superior properties, copper has been widely used as an important engineering material. Nonetheless, copper is chemically reactive and liable to corrosion in its surrounding environment[19], which limits its applications. In recent years, several researchers have focused attention on investigation of surface properties of copper. Among these, our group recently reported work on copper superhydrophobic surface, prepared by organic stearic acid passivation[20]. In this work, the presence of the flower-like surface morphology ensured a low surface energy copper stearate films that resulted in a water contact angle of 153±2° with excellent water roll-off properties[20].This resulted in higher corrosion resistance compared to the as-received bare copper surface[21].

In recent years, electrodeposition process using inorganic ions such as Mn^{2+}, Ni^{2+}, Co^{2+},Mg^{2+}in an organic electrolyte has been reported to fabricate superhydrophobic surfaces [22–26]. However, the fabricated thin films or coatings did not satisfy the industrial requirements towards cost-effectiveness, stability and anti-corrosion properties. So, the combinations of organic-inorganic coatings could help to achieve improved properties over the traditional coatings [27]. The maximum contact angle of cathodic superhydrophobic copper surface deposited from manganese chloride and myristic acid by Zhi et al. [22] has been reported to have 163° with the rolling angle of less than 3°. Similarly, nickel stearate/nickel hydroxide [23] and cobalt stearate thin films[25] have been reported to have active corrosion protection for aluminum alloy substrates.

In a recent year, one-step process electrodeposition process were used to fabricate superhydrophobic surfaces on metal surfaces. A rapid one-step method was used to fabricate a superhydrophobic surface on a magnesium alloy using an ethanol solution containing cerium nitrate hexahydrate and myristic acid [28, 30].The superhydrophobic surface shows excellent performance of corrosion resistance when immersed in corrosive aqueous solutions such as 3.5 wt % NaCl, Na_2SO_4, $NaClO_3$, and $NaNO_3$. The superhydrophobic coating based on cerium on aluminum substrate is found to be possessed anticorrosion properties [29]. Furthermore, Mn-based superhydrophobic surfaces were fabricated in the similar process and found these surfaces could be used for both corrosion resistance and antibacterial applications [31].

Several methods such as physical vapor deposition, plasma spray coating and dip coating have been utilized to fabricate Al based coatings[32-34]. Compared to these techniques, electrodeposition approach shows simplicity and better control over thickness [35].

Aluminum has been used not only as base materials but also as a protective layer due to its low density, high corrosion resistance, good formability, negative electrochemical potential, and environmental friendliness[36–38].Hence in this work, a simple electrodeposition of aluminum-based films using aluminum isopropoxide ($C_9H_{21}O_3Al$: coded as AlO_x) and stearic acid (SA)has been used to fabricate superhydrophobic thin films on copper substrates. The various molar ratios of AlO_x/SA are investigated and their respective superhydrophobic and anticorrosion properties have been discussed in this work.

Experimental:

Materials and methods:

Two pieces of copper substrates (1×2 inches) were used as cathode and anode electrodes with the working area of (1×1 inch).The as-received bare copper substrates were ultrasonically cleaned in soap solution to remove oil or grease consequently washed with deionized water and dried in an oven at 70 °C. The appropriate amount of isopropanolic solution of aluminum isopropoxide (AlO_x) ($[(CH_3)_2CHO]_3Al$) and ethanolic stearic acid (SA) ($CH_3(CH_2)_{16}COOH$) were used as an electrolyte with the respective molar ratios for deposition process. The electrochemical deposition was carried out at room temperature in 30 V of DC supply for 10 minutes. From our

previous work by Y. Huang et.al[21], has provided the inference on DC voltage. During the electrodeposition process, under constant voltage, these two electrodes were separated in parallel to each other by a distance of 1.5 cm. Different concentrations of the electrolyte solutions were prepared with the controlled AlO_x/SA molar ratios of 0, 0.05, 0.1, 0.2, 0.33, 0.4 and 0.5. The solutions were ultrasonically mixed for 10 minutes before electrodeposition. The volume of the electrolyte solution was fixedat60 ml in all cases. The coating took place at the cathodic copper electrode. After the electrodeposition, the thin films on cathodic copper substrates were carefully removed from the electrolyte solution and dried on a hot plate at 70 °C for 8 hours in an air environment.

Characterization techniques:

The surface morphology and chemical features were studied by scanning electron microscope (SEM) equipped with energy dispersive X-ray spectroscopy (EDS). The structure and chemical compositions were analyzed by Attenuated Total Reflectance-Fourier transform infrared spectroscopy (ATR-FTIR). The surface wettability analysis was carried out by First Ten Angstrom contact angle goniometer. The root mean square (rms) roughness measurement was executed by MicroXAM-100 h 3D surface profilometer. The electrochemical experiments were performed in 3.5 wt % NaCl using PGZ100 potentiostat[11, 25]. The standard three-electrode systems were used with an Ag/AgCl reference electrode, a platinum mesh as the counter electrode, and fabricated thin films as working electrode. EIS

measurements were conducted over the frequency range from 100 kHz to 10 mHz with a sinusoidal signal amplitude of 10 mV with respect to stable open circuit potential (OCP). The OCP was monitored approximately 20 hours before performing EIS. The Zview tool was used to simulate the process of electrochemical impedance after EIS measurement, which provided the fitted values of constant phase element, capacitance and charge transfer resistance as well as resistance of the electrolyte. The potentiodynamic polarization curves were scanned from -250 mV to 1000 mV with respect to OCP (vs Ag/AgCl) with a scan rate of 2 mV/s.

Results and discussion:

Fig.1 shows the morphological features of the surface of a bare copper and aluminum based (AlSA) thin films on copper substrates with various molar ratios of AlO_x/SA SEM images. The inherent rolling lines on copper substrates, which are commonly seen on rolled sheets are observed in Fig. 1 (a) and (b).The water contact angle on the surface of bare copper was found to be 94 ± 3° (see the inset of Fig. 1 (b)). The morphology of the AlSA thin films on copper substrates are presented in Fig.1 (c-j) with various molar ratios of AlO_x/SA in electrolyte solution. The morphologies are strongly influenced by the ratio of AlO_x/SA on electrodeposited thin films. When the molar ratio is low (0.05), the deposited thin film is found to be uniform on the copper substrate. The corresponding water contact angle was observed as 153 ± 1° as shown in the inset of Fig 1(d). Similarly, higher the molar ratio of AlO_x/SA resulted increased water contact angle of the deposited AlSA thin films. The water contact angle increased to 161±1° on the thin films when AlO_x/SA ratio was 0.33 in the beaker. An

observation of the formation of cracks in films appears with the molar ratio of 0.5 in the electrolyte. The water contact angle of this surface is found to be 154±1°

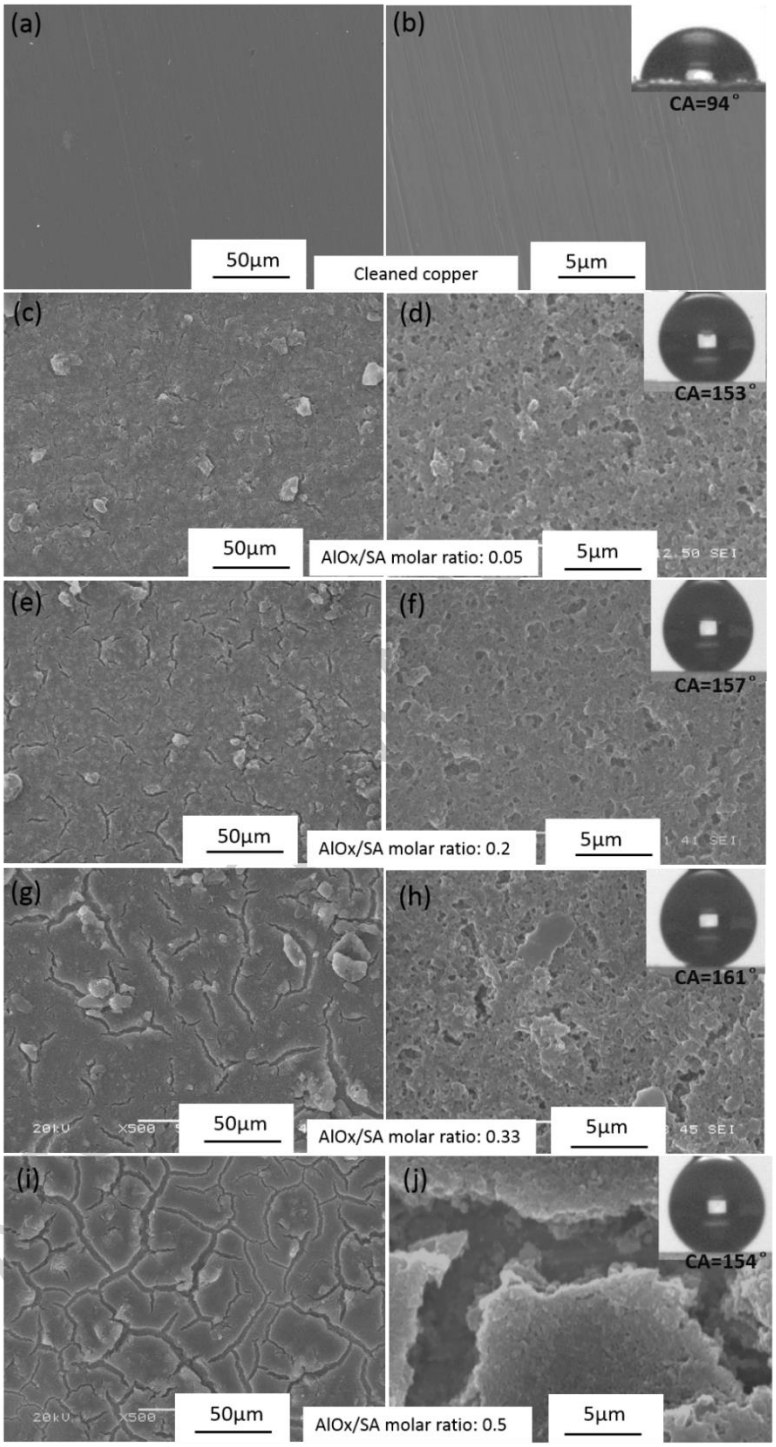

Fig. 1. SEM images of (a-b) bare copper substrate and superhydrophobic AlSA thin films with various AlO_x/SA molar ratios of (c-d) 0.05, (e-f) 0.2, (g-h) 0.33, (i-j) 0.5. The insets show the corresponding water contact angle images of droplets.

The possible mechanism of aluminum stearate (AlSA) formation is as follows:

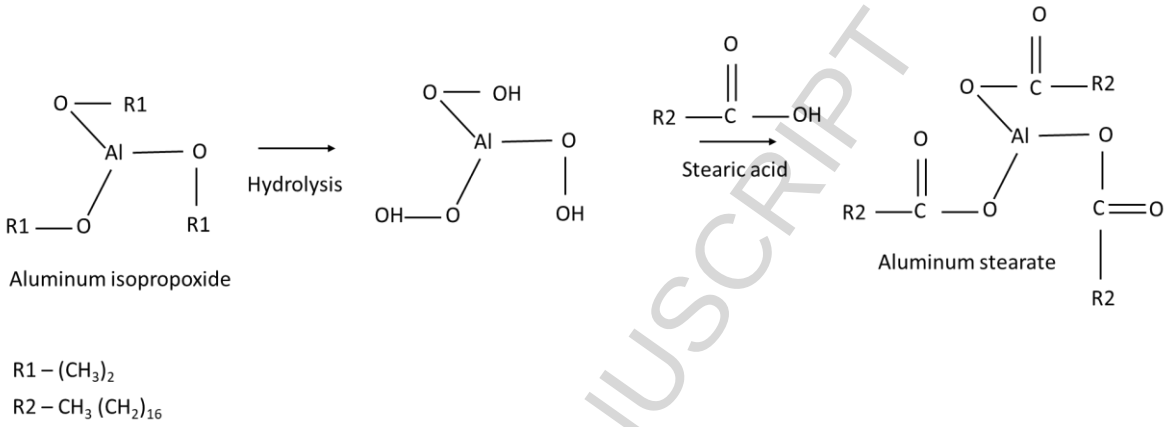

Fig. 2. Schematics of chemical reaction on the formation of aluminum stearate

In Fig. 2, dissolving the aluminum isopropoxide with propanol solution and their atmospheric hydrolysis resulted in the formation of intermediate aluminum hydroxide. The addition of ethanolic stearic acid could result in the formation of aluminum stearate (AlSA) structures.

The observed elements such as carbon, oxygen, aluminum and copper were measured by energy dispersive X-ray spectroscopy (EDS) analysis as shown in Fig. 3 (a). The EDS graphs were plotted for different molar ratios of AlO_x/SA against the energy vs intensity. Fig 3 (b) shows the increase of aluminum in the thin film's composition with respect to increase in the AlO_x/SA molar ratio (0.05, 0.2, 0.33, 0.4 and 0.5) in the electrolyte. The tendency for increase of Al atomic percentage is related with the increase in AlO_x in the electrolyte. The presence of C and O in the coating might be

related to the SA as the alkyl with the AlO_x may remain in the solution according to the reaction as presented in Fig. 1.

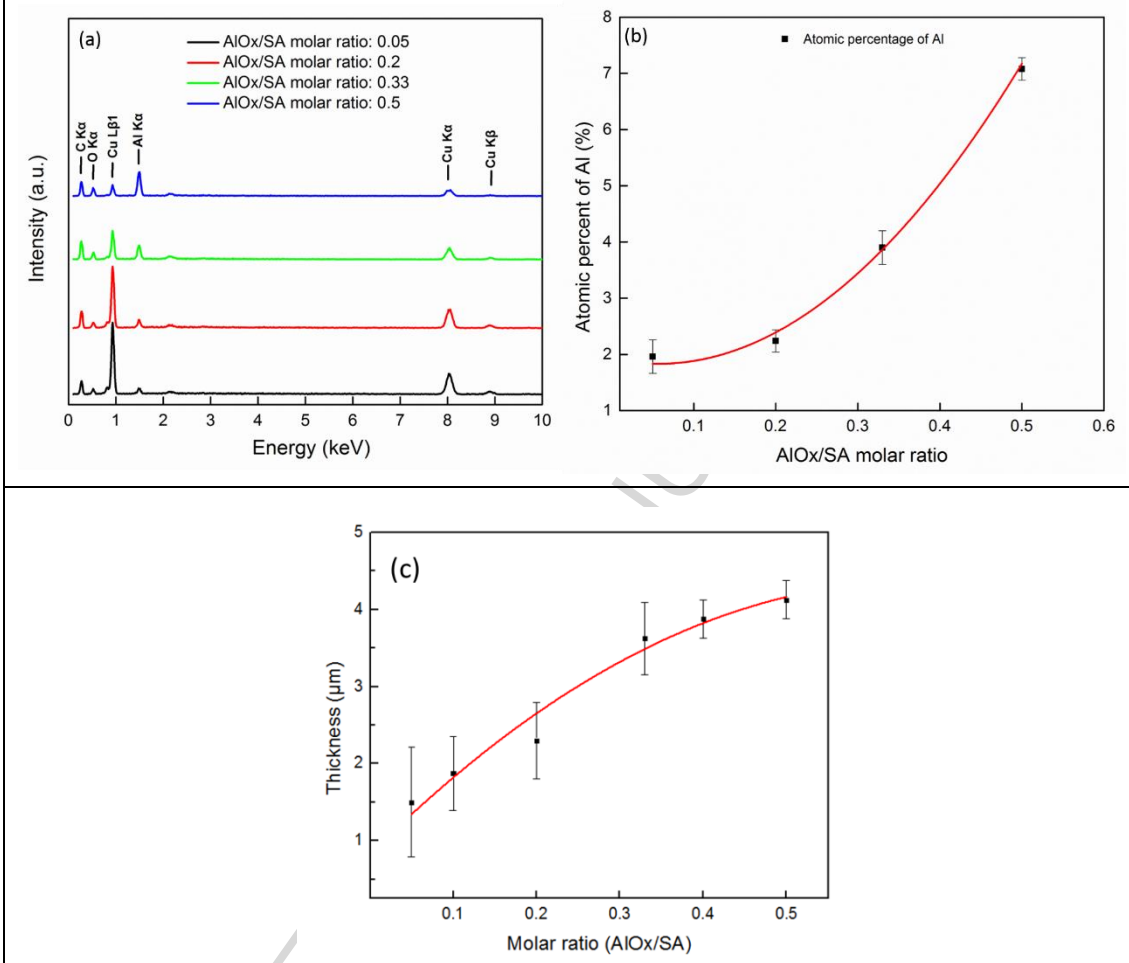

Fig.3. (a) EDS spectra of the AlSA thin film with the various molar ratios of AlO_x/SA (0.05, 0.2, 0.33, 0.5)(b) the evolution of Al percentage with respect to the AlO_x/SA molar ratio, and (c) Variation of thickens with ratio various molar ratios of AlO_x/SA

This could be due to the increase in Al-O formation. For the 0.33 AlO_x/SA, the amount of aluminum was observed as 3.9 at. %. Compared to 0.33 molar ratio coatings, the amount of observed aluminum was higher in 0.5 coatings. This is related to formation of thick films, which resulted from the increased amount of aluminum on

copper surfaces. The ratio of Al/(C+O) in an ideal film composed of AlSA would be 0.05. The closest experimental asset value by EDS is found to be 0.045. Increase of the molar ratio of AlO_x/SA in the electrolyte 0.5 leads to the increases in Al/(C+O) ratio to 0.0622. Fig. 3 (c) shows the variation of thickness with the increase of molar ratio in the electrolyte. It is found that the thickness of the films increases with the increase of the AlOx in the electrolyte.

Table I shows the elemental composition of aluminum-based thin films on copper substrates prepared with different molar ratios of AlO_x/SA in the electrolyte.

Table I Composition of aluminum based superhydrophobic thin films on copper with various molar ratios of AlO_x/SA in the electrolytes

AlO_x/SA	**Thin films composition (at. %)**					
molar ratio	C	O	Al	O/Al	O/C	Al/(O+C)
0.05	67.55	11.93	1.96	6.08	0.17	0.024
0.2	70.77	11.68	2.24	5.21	0.165	0.027
0.33	70.78	16.27	3.9	4.17	0.22	0.0448
0.5	65.2	21.89	5.42	4.0	0.33	0.0622

The wetting characteristics were characterized using water contact angle goniometry by measuring CA and CA hysteresis. Fig. 4 describes the relationship of surface roughness (rms), water contact angle and contact angle hysteresis of the thin films as a function of AlO_x/SA molar ratio.

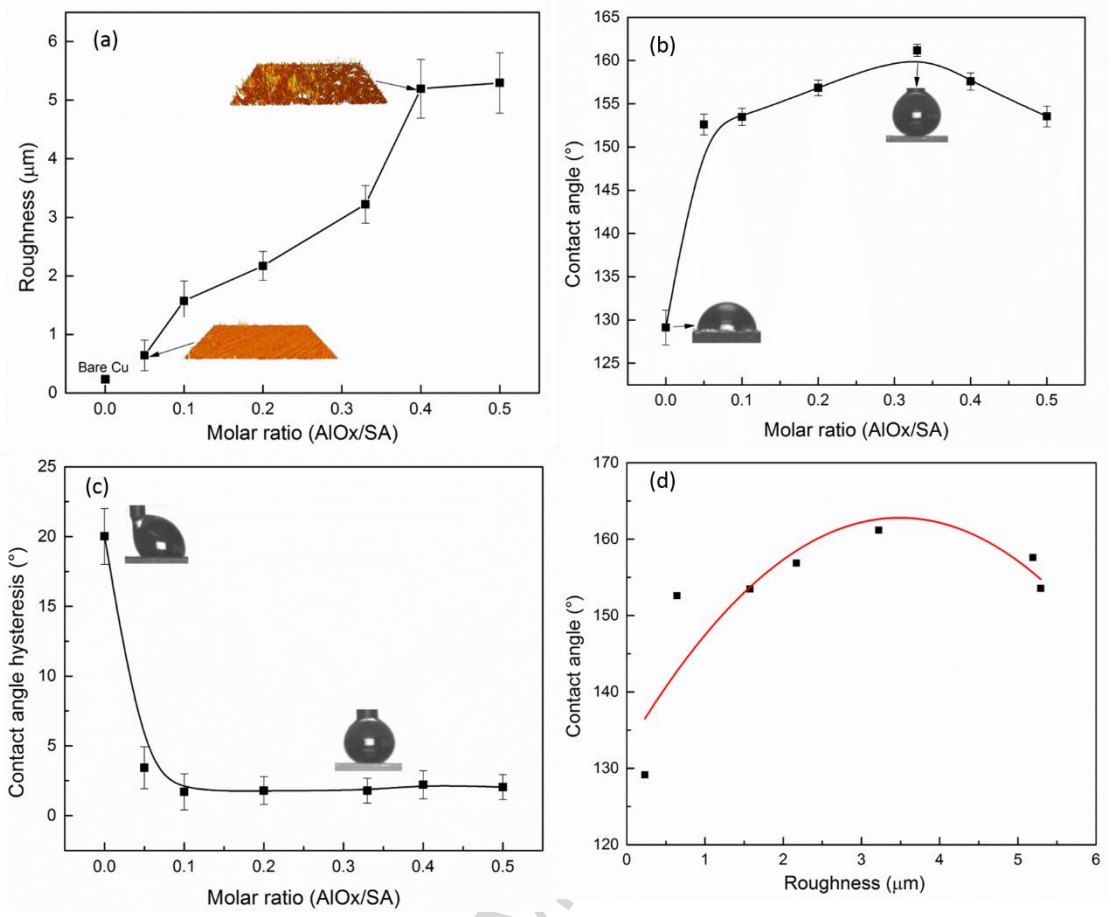

Fig.4. (a) The effect of surface roughness, (b) water contact angle (c) contact angle hysteresis with respect to various AlO_x/SA molar ratios (0.05, 0.2, 0.33, 0.5)and (d) the effect of roughness vs contact angle.

The surface roughness of bare copper surface is ~0.2 μm as shown in Fig.4 (a). In contrast, the roughness of AlSA thin films is found to be higher than that of as-received copper substrate. The roughness of the film is found to be ~5 μm prepared with the0.33molar ratio of AlO_x/SA. Raising the concentrations 0.4 and above, the roughness is increased with formation of cracks on the surface. The roughness of superhydrophobic copper stearate thin films on anodic copper substrate was reported to be 6 μm [21].In the present work, the AlSA thin films resulted in surface roughness of 3 μm, with improved superhydrophobicity. In Fig.4 (b), the contact

angle was plotted against respective AlO_x/SA. A maximum of CA was found to be at the ratio of 0.33. Interestingly, in this work the contact angles of all the copper substrates with AlSA have higher values than the anodic copper surfaces modified with only stearic acid by our previous work of Huang *et al.*[21]. Moreover, the time of electrodeposition was only 10 minutes with the potential of 10 V as compared to 120 minutes in 30 V by Huang *et al*. The superhydrophobicity of all the AlSA thin films can be attributed to the formation of dense uniform aluminum stearate structure with different morphologies (see Fig. 1). When the AlO_x/SA molar ratio is infinite (i.e., absence of stearic acid in the electrolyte solution), the contact angle of the cathodic surface decreased to 92 ± 1°,possibly due to the formation of oxides of aluminum. This value is almost equal to that of the bare copper surface. This observation clearly indicates that the presence of stearic acid with aluminum isopropoxide is responsible for achieving the superhydrophobicity on copper surfaces. Previously, we have fabricated several superhydrophobic surfaces with the combination of metal ions and stearic acid by electrodeposition such as CuSA[11], NiSA [23]and CoSA[25]. In this work, AlO_x was used as the source for Al to achieve superhydrophobic coppers providing very similar water CA.

The addition of aluminum in stearic acid increases the ability to repel the water from its surface on modified copper substrates irrespective of the molar ratio of AlO_x/SA. However, the optimum ratio of 0.33 outperformed in terms of contact angle. The corresponding hysteresis ((θ_A- θ_R) where, θ_A is advancing angle and θ_R is receding angle [39])plot against molar ratio complements the above results with 2°

(see Fig.4 (c)). In this study, the copper surfaces deposited with the small amount of AlO_x addition (less than 0.5) demonstrates superior superhydrophobicity.

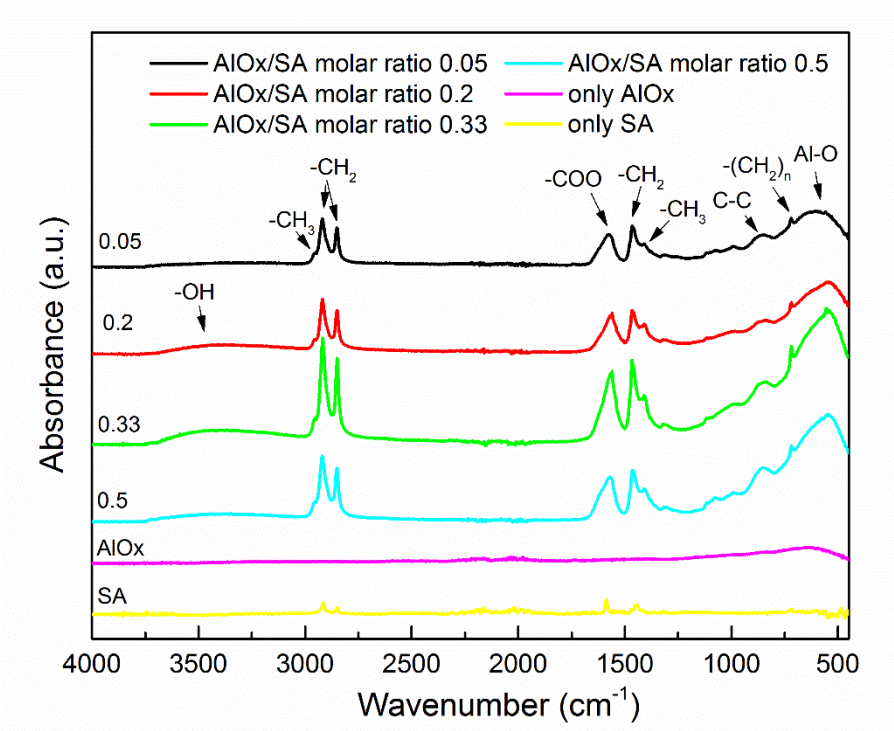

Fig.5. FTIR spectra of superhydrophobic AlSA thin films with various AlO_x/SA molar ratios (0.05, 0.2, 0.33, 0.5), with stearic acid (only SA) and without stearic acid (only AlO_x)

The chemical compositions of the AlSA superhydrophobic thin films on copper substrates fabricated were studied by ATR-FTIR analysis. Fig.5 also contains the spectra of AlO_x and SA thin films on the copper substrate. At the high frequency region, the sharp peaks at 2849 and 2916cm^{-1} are attributed to -CH_2vibrations accompanied by a small peak at 2953 cm^{-1}associated to -CH_3 vibrations respectively[40]. The presence of long chain aliphatic groups of CH_2 and CH_3effectively makes the AlSA as a low surface energy material. The mid-frequency

region at 1561 $cm^{-1}$is corresponded to the carboxyl group (COO) which has shifted from its original position from1700 cm^{-1}[41]. This shift is due to the bond formation of COO-Al in AlSA thin films. The peaks at 1445, 1421 cm^{-1}and1322 cm^{-1} are well matched with (δCH)-$CH_2$and (δCH)-CH_3, respectively. Similarly, δCH absorbance at 720 cm^{-1} was related to long chains of - CH_2[23, 41]. Further the peak at 533 cm^{-1} is attributed to Al-O bond[43,44]. In comparison, the thin films with only SA do not show the presence of COO-Al and Al-O peaks at 1561[42] and 533cm^{-1} respectively.

Fig.6 shows the potentiodynamic polarization (Tafel plots) studies of the AlSA thin films on copper substrates. The corrosion potential (E_{corr}), corrosion current density (I_{corr}) and polarization resistance (R_p) are calculated from Tafel plots and presented in TableII. As described in our previous publication [25], The corrosion potential and current densities are calculated by Stern-Geary equation,

$$R_p1 = \frac{\beta a \beta c}{2.3 Icorr(\beta a + \beta c)} \qquad (2)$$

where β_a and β_c correspond to the anodic and cathodic Tafel slopes, respectively. All the corrosion parameters were ascertained using the software provided with the potentiostat.

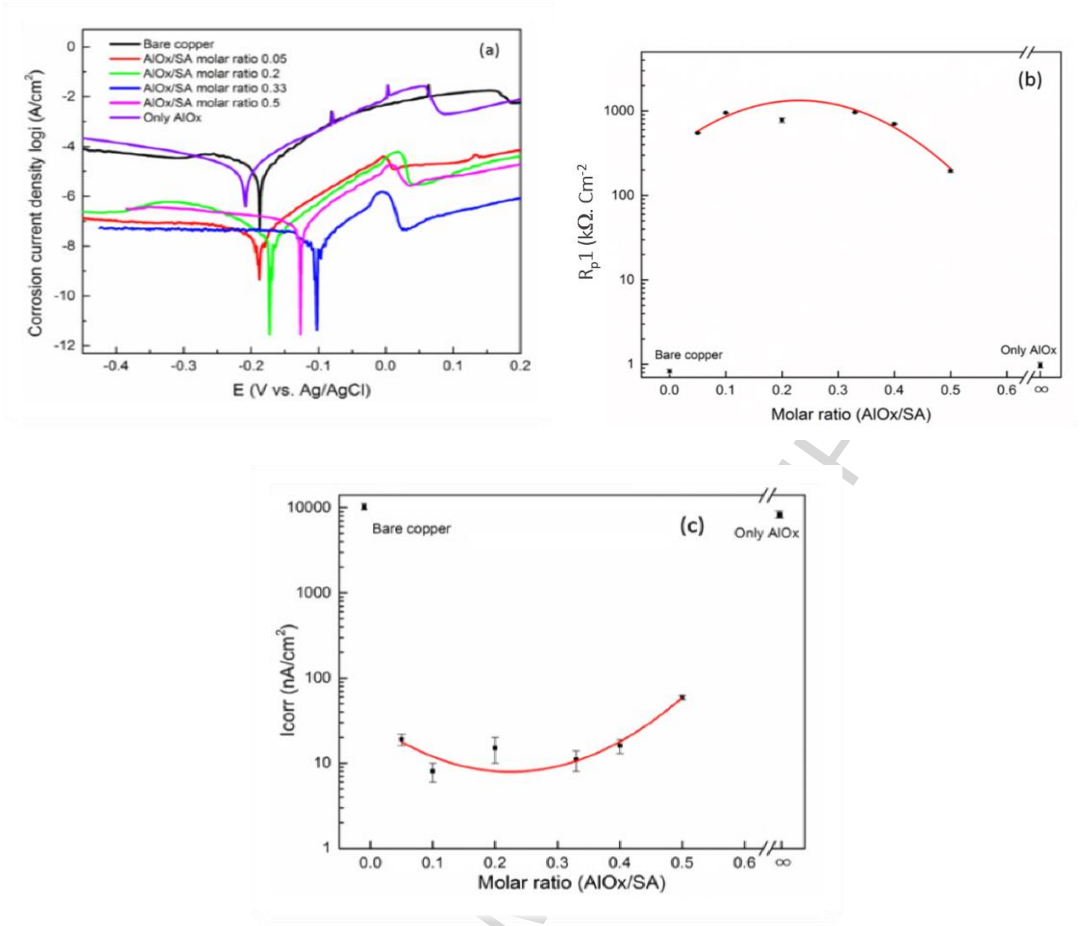

Fig.6. (a) Potentiodynamic polarization curves of superhydrophobic AlSA thin films prepared with various molar ratios ofAlO_x/SA (0.05, 0.2, 0.33 and 0.5),with stearic acid (only SA) without stearic acid (only AlO_x) compared with bare copper substrate, (b) effect of the molar ratio of AlO_x/SA on the polarization resistance R_p and (c) corrosion current density I_{corr} with respect to AlO_x/SA molar ratio.

The polarization resistance and the corrosion current density of the bare copper substrate was found to be ~1 kΩ·cm^2 and ~12.9 μA/cm^2, respectively. These results were comparable with the existing literature on corrosion data of bare copper substrates[11,25]. Fig. 6 (b) shows that R_p1 increases to the maximum of 961 kΩ·cm^{2}for the AlSA thin films prepared using the molar ratio of AlO_x/SA of 0.33. The corresponding current density was found to be the minimum of 12 nA/cm^2.In this film, the obtained R_p1 is ~1000 times higher than that of bare copper. Concurrently, the

Icorr is nearly 1000 times lower than that of bare copper. Due to the superhydrophobic nature of AlSA thin films the aqueous corrosive electrolyte does not react with it. Also, the superhydrophobic nature of thin film does not only prevents the penetration of ions from NaCl aqueous electrolyte but also inhibits the electron transfer. This leads to very low corrosion current providing the very high value of polarization resistance. In general, materials with better corrosion protection show higher polarization resistance and lower corrosion current density [15,21,23]

Table II The corrosion parameters, contact angle and charge transfer resistance of the bare copper surface with respect to various AlO_x/SA molar ratios

AlO_x/SA molar ratio	**E_{corr} (mV) With respect to Ag/AgCl**	**I_{corr} (nA/cm^2)**	***R_p1 ($k\Omega \cdot cm^2$)**	****R_p2 ($k\Omega \cdot cm^2$)**	**CA (°)**	**R_{ct} ($k\Omega \cdot cm^2$)**
Bare Cu	-189	12904	1	1.1	94	5
0.05	-195	19	549	645	153	3000
0.2	-172	18	487	444	157	1700
0.33	-105	12	961	1022	161	10000
0.5	-128	59	194	167	154	800
Only AlO_x	-213	8627	1.4	1.3	92	1.5

AlSA thin films fabricated using a higher molar ratio of 0.5of AlO_x/SA provided the polarization resistance $R_p1$and the corrosion current densities of I_{corr} are found to

be 194 kΩ·cm^2 and 59 nA/cm^2, respectively. The lesser corrosion protection could be associated with the lower contact angle of AlSA thin films. The corresponding non uniform morphologies from the SEM images in Fig 1 (i-j) support the weaker corrosion protection behavior. In the absence of stearic acid, the AlO_x based thin films R_p1 and I_{corr} are 1.4 kΩ·cm^2 and 8.6 μA/cm^2, respectively.

Ohm's law was used as an alternative approach to calculate the polarization resistance as shown in Eq (3)

$$R_p2 = \frac{\Delta V}{\Delta I} \qquad (3)$$

where ΔV and ΔI, are the variations in potential and current around E_{corr} in Tafel curve. ΔV is used with ± 15 mV.

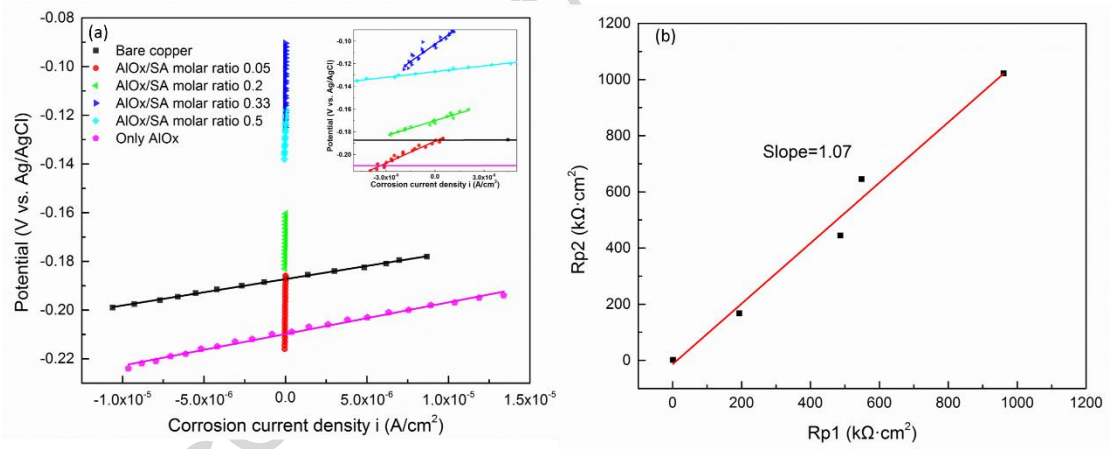

Fig.7. (a) The I-V curves with the potential variation of ± 15 mV (b) the polarization resistance (R_p) value calculated by Stern-Geary equation (R_p1) vs calculated by the Ohm's law (R_p2).

Fig.7 (a) shows the linear parts of I-V curves correspond to the Tafel plots in Fig.6(a).The I-V slopes of AlSA thin films are extremely higher as compared to bare copper substrate and pure AlO_x thin films. The calculated polarization resistances

from the Ohm's law are 1.1, 1.3 and 1022 kΩ·cm^2,correspondingto the bare copper, AlO_x based thin films and AlSA thin films prepared with the molar ratio of AlO_x/SA of 0.33, respectively. The values of polarization resistances R_p1 and R_p2 in TableII are plotted as shown in Fig.7 (b). The fitting from the slope of R_p1 vs R_p2 is ~1, which indicates the reliability of R_p values calculated in two different methods.

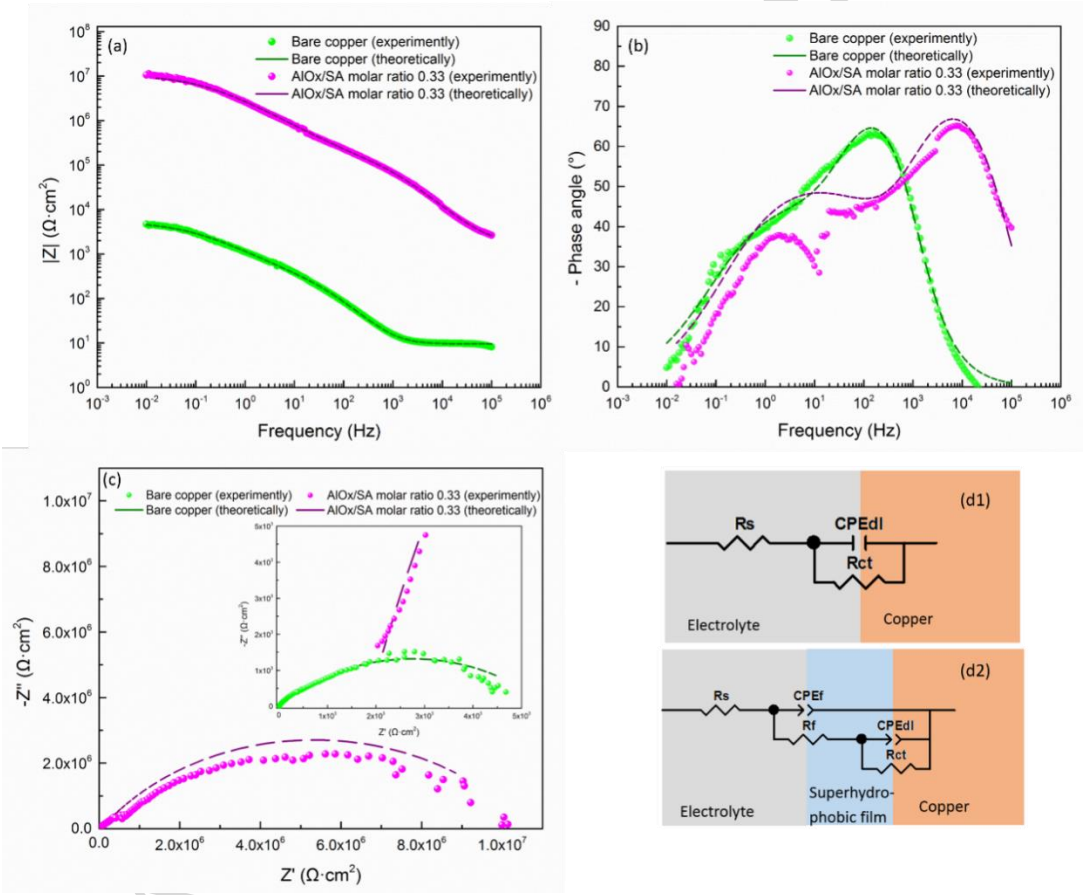

Fig.8. Electrochemical impedance spectroscopy measurements for the AlSA thin films fabricated with the molar ratio of AlO_x/SA of 0.33 and the bare copper substrate. (a) Bode modulus plot(b) Bode phase diagram (c) Nyquist plot (inset: amplified diagram at the higher frequency region) (d) equivalent circuit of (d1) bare copper (d2) superhydrophobic AlSA thin films (Dotted lines: experimental values and dashed lines :simulated values)

The EIS measurements were presented as a complementary corrosion test for the

AlSA thin films fabricated with the molar ratio of AlO_x/SA of 0.33 and bare copper substrates. The dotted lines represent the experimental values, and dashed lines correspond to simulated values shown in Fig. 8.

Fig.8 (a) shows the Bode plot of bare copper substrate and AlSA superhydrophobic thin film. In this plot |Z| has been presented with respect to frequencies. At low frequency of 0.01 Hz, the modulus of AlSA superhydrophobic thin film and bare copper substrate are found to be ~10^4k$\Omega\cdot cm^2$and 10 k$\Omega\cdot cm^2$, respectively. In the case of superhydrophobic thin film, the impedance, at both high and low frequencies, was positively shifted by three orders of magnitude. This signifies the better protection against corrosion [45],Furthermore, two peaks of superhydrophobic thin films correspond to two different time constants as shown in Bode phase plot in Fig 8(b). The high-frequency time constant at 10 kHz was assigned to its capacitance, and the low-frequency at 10 Hz was due to the capacitance of the double layer near the working electrode. The shift has been observed slightly towards a low frequency whereas in the case of bare copper substrate, only a single time constant was observed at 50 Hz. This indicates the anticorrosion properties were improved with the formation of AlSA thin films on the copper substrate.

Table III Impedance parameters of electrical equivalent circuits (EEC) and fitted EIS data of (i) solution resistance (R_s), (ii) film resistance (R_f), (iii) charge transfer resistance (R_{ct}), (iv) constant phase element (CPE).

	$R_s(\Omega\cdot cm^2)$	CPE_f		R_f ($\Omega\cdot cm^2$)	CPE_{dl}		R_{ct} ($\Omega\cdot cm^2$)
		Y_f ($\Omega^{-1}\cdot s^n\cdot cm^{-2}$)	n_f		Y_f ($\Omega^{-1}\cdot s^n\cdot cm^{-2}$)	n_f	

Copper substrate	9.7	-	-	-	2×10^{-5}	0.7	5×10^{3}
Superhydrophobic thin film on copper substrate	1.8×10^{3}	5×10^{-9}	0.9	1×10^{7}	1×10^{-7}	0.6	1×10^{5}

Fig.8 (c) shows the Nyquist plots of the AlSA thin films and the bare copper substrate, which depict the imaginary component (–Z'') vs the real component (Z'). The Nyquist plot has shown with the three different distinct resistance features such as solution resistance (R_s), film resistance (R_f) and charge transfer resistance (R_{ct}). The initial impedance value corresponds to the resistance of the electrolyte solution R_s, and for bare copper substrate it is 9.7 $\Omega\cdot cm^2$, while for superhydrophobic thin film, R_s was found to be1.8 $k\Omega\cdot cm^2$. The gain in the value is due to the presence of an additional layer (AlSA thin film).Two semicircles were observed in the Nyquist plot of AlSA thin films. The first semicircle at high frequencies, close to the origin of the plot, indicates the charge transfer resistance (R_{ctf}), and the second large semicircle apparently covers the whole frequency zone is due to the resistance of the thin film (R_f). This resistance is due to the dielectric properties of the superhydrophobic thin films. It must be mentioned that the dielectric thin film associated with the capacitance value, will be discussed later in this paragraph. The charge transfer resistance of superhydrophobic AlSA thin film (R_{ctf}) was found to be 13 $k\Omega\cdot cm^2$ and the second semicircle has a diameter of 10 $M\Omega\cdot cm^2$which is due to the resistance of the film. In contrast, the bare copper substrate shows the charge transfer resistance, R_{ct0}, value of 5 $k\Omega\cdot cm^2$as presented in the inset of Fig 7(c) (in green color). The

higher R_{ctf} and higher R_f together provide better corrosion protection properties of superhydrophobic thin film[46]. Fig.8 (d1) and (d2) are the equivalent circuits of the experimental impedance spectroscopy data of bare copper substrate and superhydrophobic AlSA thin film. The obtained experimental values of resistance and capacitance (dashed lines) are well matched with the simulated theoretical values, as presented in Table III.

The electrical equivalent circuits as shown in Fig. 8 (d) are used to fit the EIS data for the bare and superhydrophobic thin film coated copper substrates. The detailed information on equivalent circuits are described in our previous publication [25].

The inhibition efficiency (η) of the superhydrophobic film can be defined by the following equation:

$$\eta = \frac{R_{sh} - R_{ct0}}{R_{sh}} \times 100\% \quad (4)$$

$$R_{sh} = R_{ctf} + R_f \quad (5)$$

where in Eq. (5), R_{sh} is the sum of charge transfer resistance and film resistance of superhydrophobic AlSA thin films and R_{ct0} is the charge transfer resistance of the bare copper substrate. In our study, the inhibition efficiency is calculated as 99.95% with the R_{sh} is 10 MΩ·cm^2 and R_{ct0} as 5 kΩ·cm^2.

The various metal ions and stearic acid (SA) were used to fabricate superhydrophobic thin films to protect metals [11,15,21,25,47,48].Superhydrophobic thin films fabricated using Ni ions[23] and SA on aluminum substrates provided the polarization resistance (R_p) of ~ 861 kΩ·cm^{2}and total impedance (R_{sh}) (charge

transfer resistance and film resistance)) from EIS spectroscopy resulted as ~ 16 $M\Omega \cdot cm^2$. Similarly, Co ions[25] with SA complemented the R_p of 1591 $k\Omega \cdot cm^2$ and R_{sh} of 8 $M\Omega \cdot cm^2$. In this work, novel aluminum source, i.e., aluminum isopropoxide, instead of metal ions was used to fabricate Al-based superhydrophobic (AlSA) thin films on copper substrates. The obtained R_p and R_{sh} are 961 $k\Omega \cdot cm^2$ and 10 $M\Omega \cdot cm^2$, respectively. These results are similar to the reported values on aluminum substrates.

Thus, the current work by a simple electrodeposition method with controlled molar ratio of AlO_x/SA has showed higher contact angle of 161˚ with the better corrosion protection on copper surface. The addition of stearic acid in AlSA thin film is an influencing phenomenon to achieve the better corrosion protection of the copper substrate.

Fig 9 demonstrates the corrosion stability of the superhydrophobic AlSA thin film by monitoring ATR-FTIR spectroscopy of the sample before and after the corrosion test. There is a slight loss in the overall intensity of the spectrum after corrosion, which indicates the AlSA superhydrophobic thin films protect the copper surface against corrosion.

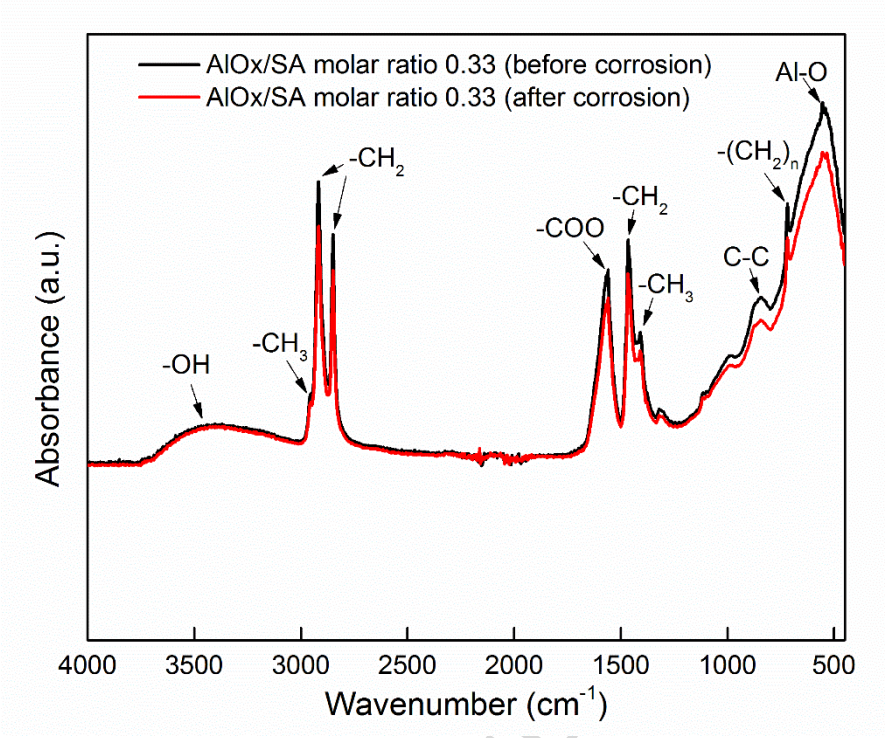

Fig.9. FTIR spectra of superhydrophobic AlSA thin films prepared with AlOx/SA molar ratio of 0.33 before and after corrosion test

Fig.10 (a) and (b) shows the high magnification SEM images of superhydrophobic AlSA thin film before and after the corrosion test. The corresponding insets represent the image of water contact angle. There were no significant changes observed on the morphology after the corrosion test. Fig.10 (c) shows the corresponding EDS spectra and photograph of superhydrophobic AlSA thin films on the copper substrate. Similar to the composition analysis from FTIR analysis, there are no changes observed from the EDS spectra after the corrosion test. Both composition and morphological analysis support the findings from the electrochemical characterization of active corrosion protection of superhydrophobic AlSA thin film.

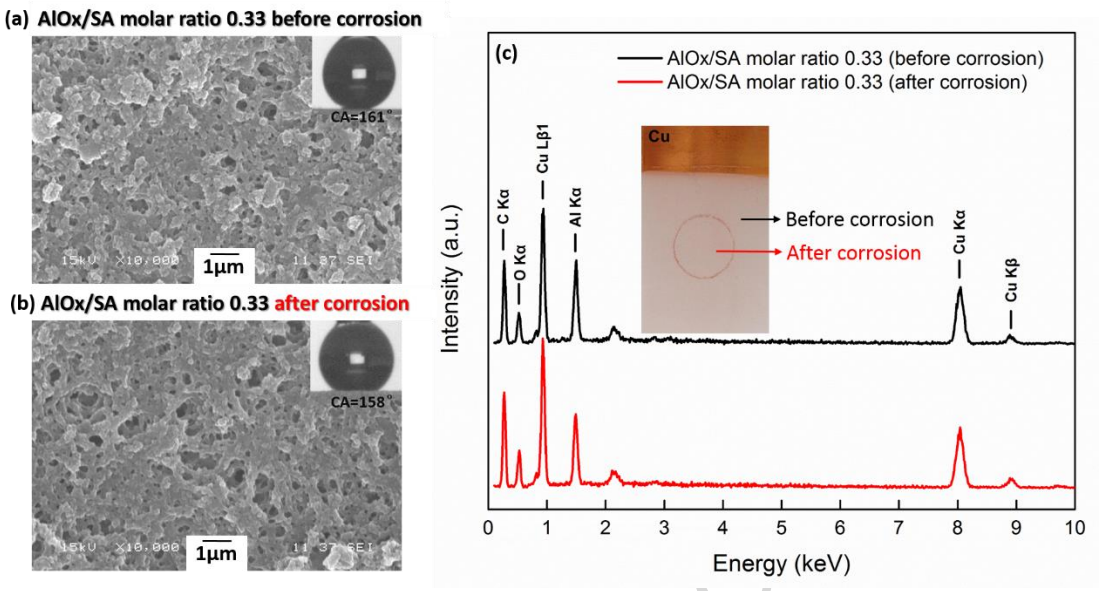

Fig.10. SEM images of AlSA thin films with the AlO_x/SA molar ratio of 0.33 (a) before corrosion (b) after corrosion (c) the corresponding EDS spectra

Conclusions:

A facile one-step electrodeposition process was used to fabricate aluminum based superhydrophobic thin films on copper substrates. The thin films were fabricated with the mixture of aluminum isopropoxide (AlO_x) and stearic acid (SA) in an ethanolic solution with various molar ratios. Composition analysis confirmed the formation of aluminum stearate (AlSA) thin films. The morphologies of the AlSA thin films were strongly influenced by the molar ratio of AlO_x/SA in the electrolyte. The AlSA thin film fabricated with 0.33 molar ratio of AlO_x/SA resulted the best superhydrophobic roll-off properties with the water contact angle of 161 ± 1° and a contact angle hysteresis of 2 ± 1°. The best superhydrophobic AlSA thin films displays the polarization resistance of 961 kΩ·cm^2, which was nearly1000 times higher than the bare copper substrate. In addition to polarization resistance, the real part of impedance

from EIS spectroscopy has been used to determine the inhibition efficiency of the superhydrophobic thin film, which was found to be 99.95 %.

Acknowledgement:

This project was supported by Natural Science and Engineering Research Council of Canada (NSERC),Karthikeyan Rajan is thankful to FRQNT for the Bourse de postdoctorat Québec-Inde (Ministère de l'Éducation et de l'Enseignement supérieur - MEESR) postdoctoral fellowship. Finally, we thank Mr. Henry Agbe for the critical reading of the manuscript.

References:

[1] X. Tian, T. Verho, R.H.A. Ras, Moving superhydrophobic surfaces toward real-world applications, Science (80-.). 352 (2016) 142–143. doi:10.1126/science.aaf2073.

[2] Y.L. Zhang, H. Xia, E. Kim, H.B. Sun, Recent developments in superhydrophobic surfaces with unique structural and functional properties, Soft Matter. 8 (2012) 11217–11231. doi:10.1039/c2sm26517f.

[3] T.M. Schutzius, S. Jung, T. Maitra, G. Graeber, M. Köhme, D. Poulikakos, Spontaneous droplet trampolining on rigid superhydrophobic surfaces, Nature. 527 (2015) 82–85. doi:10.1038/nature15738.

[4] Y. Lai, Y. Tang, J. Gong, D. Gong, L. Chi, C. Lin, Z. Chen, Transparent superhydrophobic/superhydrophilic TiO 2-based coatings for self-cleaning and

anti-fogging, J. Mater. Chem. 22 (2012) 7420–7426. doi:10.1039/c2jm16298a.

[5] Z. Zuo, R. Liao, X. Zhao, X. Song, Z. Qiao, C. Guo, A. Zhuang, Y. Yuan, Anti-frosting performance of superhydrophobic surface with ZnO nanorods, Appl. Therm. Eng. 110 (2017) 39–48. doi:10.1016/j.applthermaleng.2016.08.145.

[6] L.B. Boinovich, A.M. Emelyanenko, V.K. Ivanov, A.S. Pashinin, Durable icephobic coating for stainless steel, ACS Appl. Mater. Interfaces. 5 (2013) 2549–2554. doi:10.1021/am3031272.

[7] Y.B. Park, H. Im, M. Im, Y.K. Choi, Self-cleaning effect of highly water-repellent microshell structures for solar cell applications, J. Mater. Chem. 21 (2011) 633–636. doi:10.1039/c0jm02463e.

[8] M. Nosonovsky, Slippery when wetted, Nature. 477 (2011) 412–413. doi:10.1038/477412a.

[9] M.A. Samaha, H.V. Tafreshi, M. Gad-el-Hak, Superhydrophobic surfaces: From the lotus leaf to the submarine, Comptes Rendus - Mec. 340 (2012) 18–34. doi:10.1016/j.crme.2011.11.002.

[10] T. Sun, H. Tan, D. Han, Q. Fu, L. Jiang, No platelet can adhere-largely improved blood compatibility on nanostructured superhydrophobic surfaces, Small. 1 (2005) 959–963. doi:10.1002/smll.200500095.

[11] N. Xu, D.K. Sarkar, X. Grant Chen, H. Zhang, W. Tong, Superhydrophobic copper stearate/copper oxide thin films by a simple one-step electrochemical process and their corrosion resistance properties, RSC Adv. 6 (2016) 35466–

35478. doi:10.1039/c6ra01944g.

[12] M.F. Montemor, Functional and smart coatings for corrosion protection: A review of recent advances, Surf. Coatings Technol. 258 (2014) 17–37. doi:10.1016/j.surfcoat.2014.06.031.

[13] A.M.A. Mohamed, A.M. Abdullah, N.A. Younan, Corrosion behavior of superhydrophobic surfaces: A review, Arab. J. Chem. 8 (2015) 749–765. doi:10.1016/j.arabjc.2014.03.006.

[14] Y. Huang, D.K. Sarkar, X. Chen, Fabrication of Corrosion Resistance Micro-Nanostructured Superhydrophobic Anodized Aluminum in a One-Step Electrodeposition Process, Metals (Basel). 6 (2016) 47. doi:10.3390/met6030047.

[15] W. Xi, Z. Qiao, C. Zhu, A. Jia, M. Li, The preparation of lotus-like super-hydrophobic copper surfaces by electroplating, Appl. Surf. Sci. 255 (2009) 4836–4839. doi:10.1016/j.apsusc.2008.12.012.

[16] H. Yang, Y. He, Z. Wu, J. Miao, F. Yang, Z. Lu, Fabrication of a superhydrophobic and high-glossy copper coating on aluminum substrates, Appl. Surf. Sci. 433 (2018) 1192–1196. doi:10.1016/j.apsusc.2017.10.130.

[17] M. Gao, W. Lu, B. Yang, S. Zhang, J. Wang, High corrosion and wear resistance of Al-based amorphous metallic coating synthesized by HVAF spraying, J. Alloys Compd. 735 (2018) 1363–1373. doi:10.1016/j.jallcom.2017.11.274.

[18] D. Wu, Z. Guo, Robust and muti-repaired superhydrophobic surfaces via

one-step method on copper and aluminum alloys, Mater. Lett. 213 (2018) 290–293. doi:10.1016/j.matlet.2017.11.094.

[19] S. Kim, T.H. Le, C.S. Park, G. Park, K.H. Kim, S. Kim, O.S. Kwon, G.T. Lim, H. Yoon, A solution-processable, nanostructured, and conductive graphene/polyaniline hybrid coating for metal-corrosion protection and monitoring, Sci. Rep. 7 (2017) 1–9. doi:10.1038/s41598-017-15552-w.

[20] Y. Huang, D.K. Sarkar, X.G. Chen, A one-step process to engineer superhydrophobic copper surfaces, Mater. Lett. 64 (2010) 2722–2724. doi:10.1016/j.matlet.2010.09.010.

[21] Y. Huang, D.K. Sarkar, D. Gallant, X.G. Chen, Corrosion resistance properties of superhydrophobic copper surfaces fabricated by one-step electrochemical modification process, Appl. Surf. Sci. 282 (2013) 689–694. doi:10.1016/j.apsusc.2013.06.034.

[22] Z. Chen, F. Li, L. Hao, A. Chen, Y. Kong, One-step electrodeposition process to fabricate cathodic superhydrophobic surface, Appl. Surf. Sci. 258 (2011) 1395–1398. doi:10.1016/j.apsusc.2011.09.086.

[23] N. Xu, D.K. Sarkar, X.G. Chen, W.P. Tong, Corrosion performance of superhydrophobic nickel stearate/nickel hydroxide thin films on aluminum alloy by a simple one-step electrodeposition process, Surf. Coatings Technol. 302 (2016) 173–184. doi:10.1016/j.surfcoat.2016.05.050.

[24] G. Zhao, J. Li, Y. Huang, L. Yang, Y. Ye, F.C. Walsh, J. Chen, S. Wang, Robust Ni/WC superhydrophobic surfaces by electrodeposition, RSC Adv. 7 (2017)

44896–44903. doi:10.1039/c7ra08535d.

[25] J. Xiong, D.K. Sarkar, X.G. Chen, Superhydrophobic honeycomb-like cobalt stearate thin films on aluminum with excellent anti-corrosion properties, Appl. Surf. Sci. 407 (2017) 361–370. doi:10.1016/j.apsusc.2017.02.203.

[26] B. Zhang, J. Li, X. Zhao, X. Hu, L. Yang, N. Wang, Y. Li, B. Hou, Biomimetic one step fabrication of manganese stearate superhydrophobic surface as an efficient barrier against marine corrosion and Chlorella vulgaris-induced biofouling, Chem. Eng. J. 306 (2016) 441–451. doi:10.1016/j.cej.2016.07.062.

[27] M. Abedalwafa, F. Wang, L. Wang, C. Li, Biodegradable poly-epsilon-caprolactone (PCL) for tissue engineering applications: A review, Rev. Adv. Mater. Sci. 34 (2013) 123–140. doi:10.1016/j.progpolymsci.2013.02.003.

[28] Q. Liu, D. Chen, Z. Kang, One-step electrodeposition process to fabricate corrosion resistant superhydrophobic surface on magnesium alloy, ACS Appl. Mater. Interfaces. 7 (2015) 1859-1867. doi:10.1016/am507586u.

[29] B. Zhang, X. Zhao, Y. Li, B. Hou, Fabrication of durable anticorrosion superhydrophobic surfaces on aluminum substrates via a facile one-step electrodeposition approach, RSC Adv. 6 (2016) 35455-35465. doi:10.1039/c6ra05484f.

[30] Y. Liu, J. Xue, D. Luo, H. Wang, X. Gong, Z. Han, L. Ren, One-step fabrication of biomimetic superhydrophobic surface by electrodeposition of magnesium alloy and its corrosion inhibition, Journal of Colloids and Interface

Science. 491 (2017) 313-320. doi:10.1016/j.jcis.2016.12.022.

[31] B. Zhang, J. Li, X. Zhao, X. Hu, L. Yang, N. Wang, Y. Li, B. Hao, Biomimetic one-step fabrication of manganese stearate superhydrophobic surface as an efficient barrier against marine corrosion and Chlorella vulgaris- induced biofouling, Chemical Engineering Journal, 306 (2016) 441-451. doi:10.1016/j.cej.2016.07.062.

[32] F. Oukati Sadeq, M. Sharifitabar, M. Shafiee Afarani, Synthesis of Ti–Si–Al coatings on the surface of Ti–6Al–4V alloy via hot dip siliconizing route, Surf. Coatings Technol. 337 (2018) 349–356. doi:10.1016/j.surfcoat.2018.01.037.

[33] X. Fan, G. Darut, M.P. Planche, N. Kang, H. Liao, G. Montavon, Formation mechanisms of in-situ Al based intermetallic coatings manufactured by very-low pressure plasma spraying, Surf. Coatings Technol. 334 (2018) 300–304. doi:10.1016/j.surfcoat.2017.11.045.

[34] J. Lawal, P. Kiryukhantsev-Korneev, A. Matthews, A. Leyland, Mechanical properties and abrasive wear behaviour of Al-based PVD amorphous/nanostructured coatings, Surf. Coatings Technol. 310 (2017) 59–69. doi:10.1016/j.surfcoat.2016.12.031.

[35] T.G.S. babu and T.R. P.V. Suneesh, Electrodeposition of aluminum and aluminum-copper alloys from a room temperature ionic liquid electrolyte containing aluminum chloride and triethylamine hydrochloride, Int. J. Miner. Metall. Mater. 20 (2013) 909–916. doi:10.1007/s12613-013-0814-4.

[36] Y. Fang, X. Jiang, X.G. Sun, S. Dai, New ionic liquids based on the

complexation of dipropyl sulfide and AlCl3 for electrodeposition of aluminum, Chem. Commun. 51 (2015) 13286–13289. doi:10.1039/c5cc05233e.

[37] Y. Hou, R. Li, J. Liang, Simultaneous electropolishing and electrodeposition of aluminum in ionic liquid under ambient conditions, Appl. Surf. Sci. 434 (2018) 918–921. doi:10.1016/j.apsusc.2017.11.034.

[38] Q. Zhang, Q. Wang, S. Zhang, X. Lu, Effect of nicotinamide on electrodeposition of Al from aluminium chloride (AlCl3)-1-butyl-3-methylimidazolium chloride ([Bmim]Cl) ionic liquids, J. Solid State Electrochem. 18 (2014) 257–267. doi:10.1007/s10008-013-2269-y.

[39] H.B. (eds) Bracco . G, Contact Angle and Wetting Properties in Surface Science Techniques, 2016. doi:10.1007/978-3-642-34243-1.

[40] A. Siddaramanna, N. Saleema, D.K. Sarkar, A versatile cost-effective and one step process to engineer ZnO superhydrophobic surfaces on Al substrate, Appl. Surf. Sci. 311 (2014) 182–188. doi:10.1016/j.apsusc.2014.05.039.

[41] Barbara H. Stuart, Infrared spectroscopy, Wiley-VCH GmbH Co. KGaA. (2004) 264.

[42] Y. Guo, Y. Jin, Z. Su, Spectroscopic study of side-chain melting and crystallization of regioregular poly(3-dodecylthiophene), Polym. Chem. 3 (2012) 861–864. doi:10.1039/c2py00582d.

[43] A. Vázquez, T. López, R. Gómez, Bokhimi, A. Morales, O. Novaro, X-Ray Diffraction, FTIR, and NMR Characterization of Sol-Gel Alumina Doped with Lanthanum and Cerium, J. Solid State Chem. 128 (1997) 161–168.

doi:10.1006/jssc.1996.7135.

[44] J.T. Kloprogge, L. Hickey, R.L. Frost, FT-Raman and FT-IR spectroscopic study of synthetic Mg/Zn/Al-hydrotalcites, J. Raman Spectrosc. 35 (2004) 967–974. doi:10.1002/jrs.1244.

[45] D.I. Njoku, M. Cui, H. Xiao, B. Shang, Y. Li, Understanding the anticorrosive protective mechanisms of modified epoxy coatings with improved barrier, active and self-healing functionalities: EIS and spectroscopic techniques, Sci. Rep. 7 (2017) 1–15. doi:10.1038/s41598-017-15845-0.

[46] P.L. Bonora, F. Deflorian, L. Fedrizzi, Electrochemical impedance spectroscopy as a tool for investigating underpaint corrosion, Electrochim. Acta. 41 (1996) 1073–1082. doi:http://dx.doi.org/10.1016/0013-4686(95)00440-8.

[47] J. Liang, Y. Hu, Y. Fan, H. Chen, Formation of superhydrophobic cerium oxide surfaces on aluminum substrate and its corrosion resistance properties, Surf. Interface Anal. 45 (2013) 1211–1216. doi:10.1002/sia.5255.

[48] Z. Gong, J. Wang, L. Wu, X. Wang, G. Lü, L. Liao, Fabrication of super hydrophobic surfaces on copper by solution-immersion, Chinese J. Chem. Eng. 21 (2013) 920–926. doi:10.1016/S1004-9541(13)60569-8.

Graphical abstract:

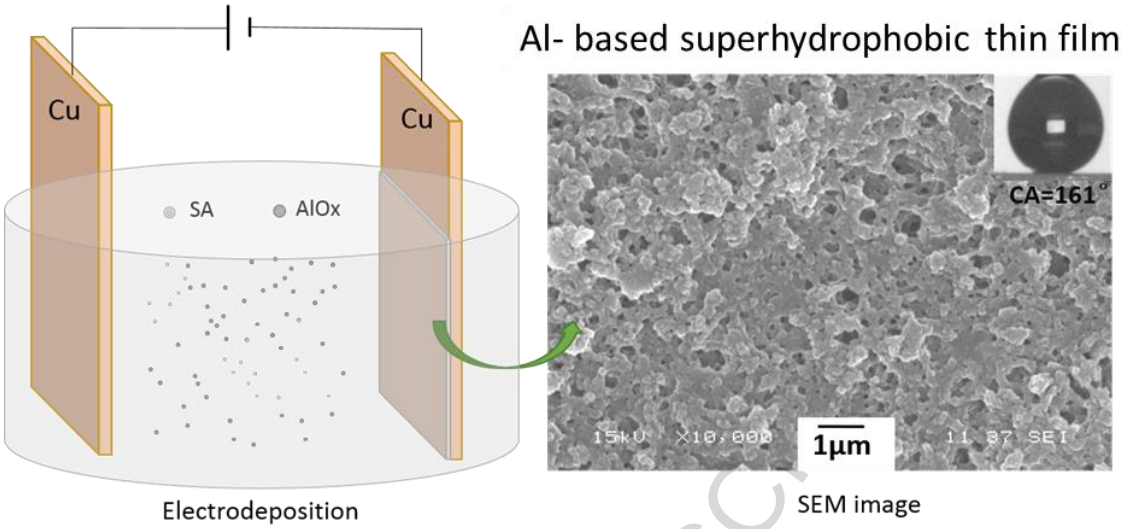

Schematic of fabrication of aluminum-based superhydrophobic thin film on copper substrate and its corresponding SEM morphology

Highlights

- One-step electrodeposition of Al-based superhydrophic thin films on copper surfaces.
- Compositional analysis by infrared and x-ray analysis confirmed the AlSA formation
- Best superhydrophobicity with the water contact angle of 161 ± 1° was obtained.
- Polarization resistance of 961 $k\Omega \cdot cm^2$ and impedance of 10 $M\Omega \cdot cm^2$ were obtained.
- Corrosion inhibition efficiency for the AlSA thin film is found to be 99.95%.